

Sediment Incipient Motion in Sewer with a Bed Deposit

Wan Hanna Melini WAN MOHTAR¹

Charles HIN JOO BONG²

Aminuddin AB. GHANI³

Mir Jafar Sadegh SAFARI⁴

Aizat Mohd TAIB⁵

Haitham Abdulmohsin AFAN⁶

Ahmed EL-SHAFIE⁷

ABSTRACT

This paper analyses experimental data on sediment incipient motion with varying sediment bed thickness (of d_{50} , 5, 10 and 24 mm). Sediment particles (with sizes ranging from 0.5 mm to 4.78 mm) were used to evaluate the effect of deposited bed. Variation of shear velocity estimation was investigated where the critical Shields parameter was expressed using bed-slope product u_{*cb} , log-law u_{*cl} and was extended in terms of critical mean velocity. The critical Shields parameters obtained were significantly lower than the traditional Shields curve when u_{*cl} was used compared to u_{*cb} . Higher critical mean velocity is needed for shallower deposits.

Keywords: Threshold criteria of sediment motion, shields parameter, sediment bed thickness.

Note:

- This paper was received on May 31, 2019 and accepted for publication by the Editorial Board on September 28, 2020.
- Discussions on this paper will be accepted by March 31, 2022.
- <https://doi.org/10.18400/tekderg.572529>

1 Universiti of Kebangsaan Malaysia, Department of Civil Engineering, Bandar Baru Bangi, Malaysia
hanna@ukm.edu.my - <https://orcid.org/0000-0002-5684-5577>

2 Universiti of Malaysia Sarawak, Department of Civil Engineering, Sarawak, Malaysia
bhjcharles@unimas.my - <https://orcid.org/0000-0001-5447-0786>

3 Universiti of Sains Malaysia, River Engineering and Urban Drainage Research Centre, Penang, Malaysia
redac02@usm.my - <https://orcid.org/0000-0002-8921-9569>

4 Yasar University, Department of Civil Engineering, Izmir, Turkey
jafar.safari@yasar.edu.tr - <https://orcid.org/0000-0003-0559-5261>

5 Universiti of Kebangsaan Malaysia, Department of Civil Engineering, Bandar Baru Bangi, Malaysia
amohdtaib@ukm.edu.my - <https://orcid.org/0000-0002-0307-3016>

6 Department of Civil Engineering, Al-Maarif University College, Ramadi, Iraq
haitham.afan@gmail.com - <https://orcid.org/0000-0002-4957-756X>

7 Universiti of Malaya, Department of Civil Engineering, Kuala Lumpur, Malaysia
elshafie@um.edu.my - <https://orcid.org/0000-0001-5018-8505>

1. INTRODUCTION

The work on incipient sediment motion have been exhaustively conducted since the pioneer work of Shields (1936). Since then, abundant research studies have looked into the phenomenon and studied it in terms of sediment characteristics and flow behaviour, including varying definitions of incipient sediment motion (Buffington and Montgomery, 1997). The accuracy of incipient sediment motion is important in determining the bedload transport (Toriman et al., 2009; Wan Mohtar et al., 2016), sediment resuspension (Wan Mohtar, 2017) and river bank erosion (Toriman et al., 2013). The most commonly used approach to obtain the threshold value for sediment motion is the Shields diagram based on sediment flux, which is an extrapolation of bed load transport rates to zero or low value. This well-established curve was developed based on homogeneous particles on a loose boundary condition. The threshold value of sediment motion can be obtained through the particle Reynolds number, often presented as $Re_* = u_{*c}d/v$, where u_{*c} is the critical shear velocity and d is the sediment size. However, with the parameter u_{*c} is in both abscissa and ordinate (from the critical bed shear stress) makes it implicit, hence, the shear velocity has been eliminated from the sediment characteristics and is presented as dimensionless grain size parameter defined by $D_* = \sqrt{g(s - 1)d^3/v}$ (Yalin, 1972). This parameter presents only the sediment and flow characteristics, eliminating the shear velocity u_{*c} from abscissa which made the interpretation of threshold criteria more straightforward to be solved explicitly.

The presence of sediment has been established to be found even in sewerage pipes, commonly described as ‘in-sewer sediment’ (Crabtree, 1989; Tait et al., 1998; Seco et al., 2018). When the flow velocity is considerably lower than the critical velocity, the sediment tends to be deposited and, overtime, accumulated to a certain depth. In particular, during dry seasons with low flow, the condition promotes long-term deposition, whereby the deposited sediment changes the surface roughness, affects the velocity distribution, reduces the flow capacity and increases hydraulic resistance (Banasik et al., 2005). In European countries, where the sewerage is often combined with storm water sewers, 90 % of the pollution load during storm events is from the accumulated in-sewer sediment (Crabtree, 1989; Schertzinger et al., 2019).

In-sewer sediments carry high loads of both organic and inorganic particles. The fraction of organic and inorganic materials in the sewer sediment mixture depends on catchment characteristics, sewer type, geometry, the type of wastewater and sanitary habits of the population (Banasik et al., 2005; Regueiro-Picallo et al., 2018). High organic content in the wastewater has high microbial community, which promotes the formation of biofilm on the accumulated sediment, particularly on a stable sediment bed surface (Vollertsen, 2000; Ahyerre et al., 2001; McLellan and Roguet, 2019). The cementing process obviously reduced the effective area of pipes, which consequently resulted in undesirable environmental complications such overflow wastewater spill particularly during storm events.

In sewer pipes, the sediment bed is better presented as rigid boundary condition and the threshold criteria might be different (Novak & Nalluri, 1975; Ashley et al., 2004; Safari et al., 2017). The deposited sediment in pipes may have thickness t_s less than 10 mm and can go up to 100 mm (Ashley et al., 1992), and can be as high as 330 mm in storm water drains (Bong et al., 2014). Even so, due to limited studies on the threshold criteria on rigid boundary conditions, in particular with bed deposits, the established Shields method is still applied in

sewerage and storm networks (Verbanck et al., 1994). Shields described the threshold movement (of a loose-boundary channel) based on shear stress approach, characterising the near bed influence through the critical shear velocity u_{*c} . However, the effect of sediment deposit thickness was not considered, and the characterisation of incipient sediment motion is rendered inaccurate, particularly with increasing deposition thickness. Furthermore, we investigate the variation of u_{*c} on threshold criteria based on two definitions, i.e. bed slope product and the logarithmic law of the wall. Despite estimation of shear stress based criteria being hydraulically correct, presenting as simple mean velocity is more useful and straightforward, particularly concerning the self-cleansing design (Novak and Nalluri, 1975; Bong et al., 2013). Thus, analysis is extended to evaluate the incipient sediment motion on various bed thicknesses, based on the mean flow velocity. This study also incorporates the results from previous work of Salem (1998) which permits a more exhaustive analysis of the influence of sediment deposits in the threshold criteria of sediment movement in a rigid boundary.

2. METHODOLOGY

The experimental works were conducted in a glass walled, tilting flume with dimensions of $0.6 \text{ m} \times 0.4 \text{ m} \times 6.3 \text{ m}$, located at the hydraulic laboratory of Universiti Sains Malaysia. The velocity and discharge values were obtained through readings from an electronic current meter, placed at the inlet of flume. The detailed experimental parameters are described in Table 1. Note that the range of slope S_0 , sediment size d_{50} and sediment thickness presented here followed the site characteristics observation by Ab. Ghani et al. (2000).

Table 1 - The experimental parameters conducted, and associated parameters related to the work of Salem (1998).

Parameter	this study	Salem (1998)
Flume width, $B(\text{m})$	0.6	0.3
Slope, S_0	1/200, 1/350, 1/500, 1/1000	1/500, 1/600, 1/750, 1/1000, 1/1200, 1/1700
Median grain size, d_{50} (mm)	0.81, 1.53, 4.78	0.55, 0.97, 1.80, 3.09, 4.78
Dimensionless grain number D_*	89.6, 232.6, 1297.0	50.6, 116.0, 289.0, 636.6, 180.6
Thickness of sediment deposit, $t_s(\text{mm})$	d_{50} , 5, 10, 24	d_{50} , 5, 10, 24

The observation section was placed about 3.5 m from the inlet, where the flow was ensured to be uniform and steady by placing a corrugated sheet stack at the front. Sediment with varying bed thickness (as described in Table 1) was filled in the observation section (with the total length up to 2.1 m) and levelled with a trowel.

The flume was slowly filled with water to minimise disturbances to the levelled sediment bed, before reaching the desired water depth. The discharge (i.e. the velocity too) was systematically increased until incipient sediment motion was observed. The definition of incipient sediment motion employed was general intermittent movement, as described by Kramer (1935). The critical mean velocity U_c that is, the velocity when the incipient sediment motion was observed, is defined as the mean (depth) averaged flow velocity.

The fundamental quantity to describe the incipient sediment motion is the dimensionless critical Shields parameter θ_c , described as,

$$\theta_c = \frac{\tau_c}{(\rho_s - \rho)gd}, \quad (1)$$

where $\tau_c = \rho u_{*c}^2$ is the critical bed shear stress, u_{*c} is the critical shear velocity, i.e. a characteristic velocity defined at the near-bed region, $d = d_{50}$ is the mean grain diameter and ρ_s and ρ are the sediment and fluid densities, respectively.

In this study, the critical shear velocity u_{*c} is presented in two forms. One is calculated through the bed-slope product, denoted as the critical shear velocity u_{*cb} was obtained using

$$u_{*cb} = \sqrt{gRS_0}. \quad (2)$$

As the mean critical velocity U_c for each set of experiments were obtained, the critical shear velocity was also calculated using the log-law layer,

$$\frac{U_c}{u_{*cl}} = \frac{1}{\kappa} \ln \frac{z}{z_0}, \quad (3)$$

whereby the critical shear velocity calculated using Equation (3) was denoted as u_{*cl} . The symbol κ is denoted as the Von Karman coefficient, taken as 0.4, z_0 is the roughness layer, calculated as $z_0 = d_{50}/30$ and $z = 0.2h$.

Novak and Nalluri (1975) (as cited in Novak and Nalluri, 1984), proposed the representation of incipient sediment motion (in terms of relative particle size (d/R)) as particle critical Froude Number F_d

$$F_d = \frac{U_c}{\sqrt{gd(s-1)}} = a \left(\frac{d}{R} \right)^b, \quad (4)$$

where U_c is the critical mean velocity (obtained at the incipient sediment motion) and R is the hydraulic radius. The coefficients a and b were found as 0.5 and -0.4, respectively. The work of El-Zaemey (1991) incorporated wider sediment sizes, and the coefficients of a and b were found as 0.75 and -0.34, respectively.

Equation (4), also known as densimetric Froude number was found to be better correlated with sediment pickup rate compared to the Shields parameter (Cheng and Emadzadeh, 2015). Taking into account past research, this study investigates the relation of $\theta_c \sim D_*$ and revisits the Equation (4) in a more robust manner. To assess the effect of thickness in a more comprehensive approach, the results obtained from this study are combined with the data

obtained from Salem (1998). The details of Salem's experimental parameters are presented in Table 1. Note that the sediment thickness employed in both studies are similar, which permits a combination of evaluation and analysis, in particular in terms of sediment size.

3. RESULTS AND DISCUSSION

3.1. Representation of the Shields Curve

Fig. 1 shows θ_c against particle Reynolds number D_* for varying slope S_0 . The modified Shields curve is also included which was calculated using the empirical function developed by Brownlie (1981), $\theta_c = 0.22D_*^{0.6} + 0.06\exp(-17.77D_*^{0.6})$. The discussion starts with Fig. 1, recalling that θ_{cb} was obtained using u_{*cb} .

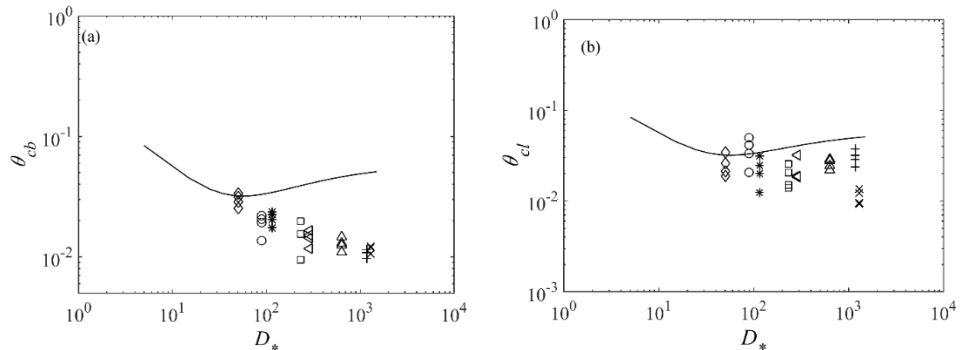


Fig. 1 - Parameter θ_c calculated using (a) bed slope product and (b) log-law. The Shields curve calculated using Brownlie (1981) is also presented, marked here as the solid line. The symbols present particle Reynolds number D_* of 50.6 (\circ), 89.6 (\circ), 116.0 (*), 232.0 (\square), 289.0 ($<$), 636.6 (\triangle), 1180.6 (+) and 1297.0 (\times).

In general, the sediment thickness plays an important role for low, dimensionless grain size, i.e. $D_* < 200$ region. A huge gap of θ_c was observed, corresponding to the sediment thickness, where higher sediment thickness requires more forces to observe the incipient sediment motion. As the particle size gets bigger, that is for $D_* > 200$, the effect of sediment thickness became insignificant where the range of θ_c became narrower. As the bed slope S_0 gets higher, the horizontal weight forces $W_x = WgS_0$ becomes more evident and contributes to the movement due to self-weight. The symbol W represents the submerged weight particle; assuming the sediment grain is spherical, W is calculated as $W = \pi(s - 1)\rho gd^3/6$. Therefore, the fluid forces needed to initiate sediment movement are less, even with the thicker sediment depth.

Most, if not the majority of the data fall well below the Shields curve. The obtained θ_{cl} are about two orders of magnitude smaller than the traditional Shields curve. The θ_{cl} obtained using the log law provides better representation compared to the ones in Fig. 1a, when the critical Shields parameter was calculated using u_{*cb} . Although the profile is rather similar, where both critical Shields parameter are low as D_* increases, the θ_{cl} consistently has a higher

value than θ_{cb} . Moreover, the θ_{cl} falls closer to the Shields line compared to θ_{cb} . This difference in the magnitude is only within the order of $[10^{-1}]$. This indicates that, for better incipient sediment motion, the shear velocity using log-law has a better approximation.

For $t_s = d_{50}$, the θ_c obtained by both methods were similar, particularly for $D_* \leq 200$ and significantly deviates for a larger particle size. However, increasing t_s to 5 mm shows that the θ_c value obtained by both methods started to depart even for $D_* \leq 200$. The difference became more apparent as the sediment thickness was increased to 10 mm and 24 mm. The deposited sediment evidently influences the value of the bottom friction factor f and increased the surface roughness of the pipe. The often-adopted depth-slope based shear stress $\tau = \rho g H S_0$ does not take into account the influence of bottom friction factor f . The mean wall shear stress calculated based on the Darcy's $\tau = \frac{1}{8} f \rho (U_c^2)$ can be more than five times compared to the (basic) type based pipe roughness when $t_s = 24$ mm.

3.2. Representation of Particle Critical Froude Number

The data of F_d against d_{50}/y_0 was plotted for each sediment size D_* . Fig. 2 shows the representation of a typical F_d - d_{50}/y_0 plot, where the effect of thickness is evident. F_d was consistently higher for the lowest t_s and steadily decreased as t_s was increased. Based on the data, the influence of t_s (as denominator) in Equation 4 proved to be more salient in the determination of the F_d parameter.

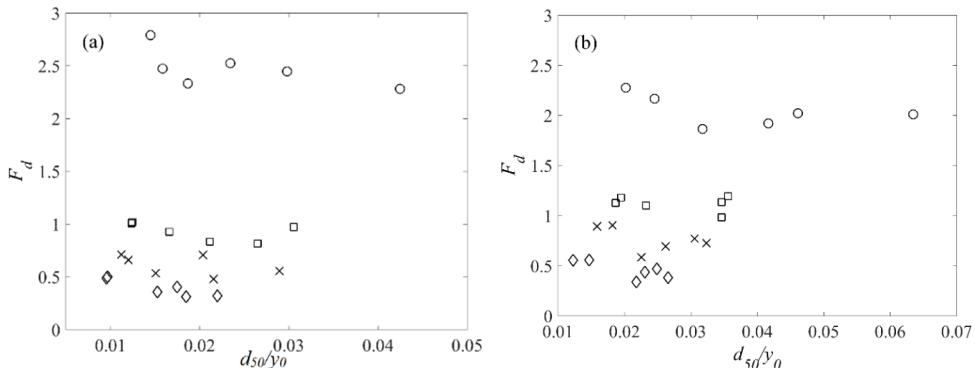


Fig. 2 - Representative plots of F_d against d_{50}/y_0 for sediment sizes d_{50} of (a) 0.55 mm and (b) 0.97 mm. Symbols represent sediment thickness D_* at d_{50} (\circ), 5 mm (\square), 10 mm (\times) and 24 mm (\diamond).

The coefficients of a and power law b were individually obtained through the power law relationship for each sediment thickness t_s and sediment size D_* using Equation (4). In this analysis, the evaluation is extended to the sediment thickness of 50 mm, where the data was taken from the work of Schvidchenko (2000). Figures 3 and 4 show the plots for $a \sim D_*$ and $b \sim D_*$, respectively.

The profile for a will be discussed first. In general, the values of a were found to be relatively constant and independent of D_* . Values of a were found around $1 < a < 2.1$, with an averaged value $a \approx 1.5$ at $t_s = d_{50}$. As the sediment thickness increases to 5 mm, a was found to be less than 1 and falls between the range of 0.5 to 1 (except for $D_* = 636$). It is acknowledged that this data may be an outlier but was included anyway in the plot to show the variation.

Increasing sediment thickness decreases the coefficient a to a lower value, where $a \approx 0.37$ for $t_s = 10$ mm. Coefficient a was found at about ≈ 0.2 when the sediment thickness is 24 mm. The sediment bed thickness of 50 mm (taken from the Schvidchenko data) was seen to have a similar trend of decreasing a (with value ≈ 0.17), but only for $D_* < 500$, whereas, above this value, a was obtained at about ≈ 0.8 .

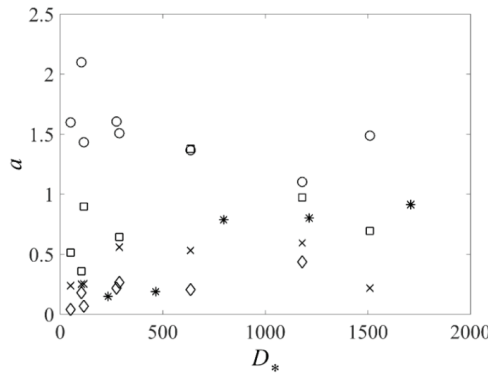


Fig. 3 - The determined coefficient a against D_* for varying sediment thickness t_s ; d_{50} (\circ), 5 mm (\square), 10 mm (\times), 24 mm (\diamond) and 50 mm ($*$).

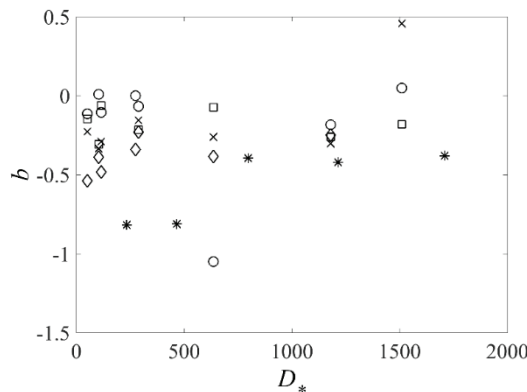


Fig. 4 - The determined coefficient b against D_* for varying sediment thickness t_s ; d_{50} (\circ), 5 mm (\square), 10 mm (\times), 24 mm (\diamond) and 50 mm ($*$).

A decreasing trend of coefficient a as sediment thickness t_s is increased, was observed. This indicates that for a fixed sediment size, the critical velocity U_c decreased as the sediment thickness increased. Thicker sediment resulted in an increase of the surface roughness on the rigid boundary, simultaneously decreasing U_c .

Next, the relationship of $b \sim D_*$ is analysed on. The profile of power law b shows a similar trend where, as t_s increases, coefficient b was found to be consistently decreased (except for $t_s = 50$ mm at high D_*), which shows an adverse pattern with coefficient a . Interestingly, the power law b was about ≈ 0.4 for $D_* > 500$ but has significantly decreased to about 0.8 for lower D_* . The summary of coefficients a and b are presented in Table 2 along with the values obtained from previous studies of Novak & Nalluri (1984) and El-Zaemey (1991). Note that the values a and b for $t_s = 50$ mm from the Schvidchenko data was omitted due to unexplainable disparities of both coefficients a and b between low and high D_* .

Table 2 - Summary of coefficients a and b for different sediment thickness t_s and comparison with values obtained from Novak & Nalluri (1984) and El-Zaemey (1991).

Study	t_s (mm)	a	b
Novak & Nalluri (1984)	1	0.5	-0.4
El-Zaemey (1991)	1.5	0.75	-0.34
this study	d_{50}	1.53	-0.18
	10	0.78	-0.18
	5	0.38	-0.26
	24	0.20	-0.38

The values of coefficient a and power law b obtained in this study were within the similar range as the values reported in the works of Novak & Nalluri (1984) and El-Zaemey (1991). Even so, it is worth highlighting that the same range of $0.3 < b < 0.4$ were obtained despite the higher t_s used in this study.

Obviously higher threshold criteria are needed for $t_s \approx d_{50}$, believed due to the hydraulically smooth behaviour at near bed. The finer sediment size, in particular, lies well within the laminar sub-viscous layer and higher fluid forces are needed to initiate movement and sediment entrainment. Within this layer, the viscous stresses are dominant and reduced the local fluid velocity. It is noted that the smaller size discussed here is $D_* = 89.6$ (i.e. 0.55 mm), which is considered medium sand and usually not associated with a hydraulically smooth region. But it is anticipated that for smaller sediment size, in particular for $d_{50} < 0.2$ mm, it will be the case.

On the other hand, increasing t_s subsequently increased the surface roughness where a hydraulically rough region is highly likely. The bed roughness inhibits the formation of the viscous sublayer, exposing the sediment particles to the near-bed turbulence, causing them to be more easily entrained (Wan Mohtar & Munro, 2013).

Fig. 3 shows that the deposit thickness is an important parameter, where the constant coefficient a value as given in Equation (4) might provide an inaccurate representation of F_d . To assess the influence of grain-bed ratio d_{50}/t_s in coefficients a and b , Fig.5 depicts plots of both coefficients with d_{50}/t_s .

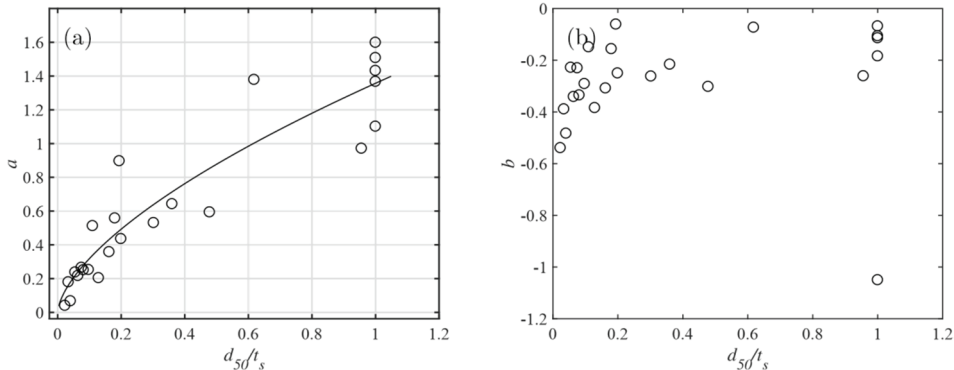


Fig. 5 - The relation of d_{50}/t_s against coefficients (a) a and (b) b .

The coefficient a increases as grain-bed ratio increases and lies within the range $1 \sim 1.6$ for $d_{50}/t_s = 1$. As $d_{50}/t_s < 1$, the value of a gradually decreases and becomes close to ~ 0 when $d_{50}/t_s \ll 1$. Based on the data, a dependency of coefficient a on the ratio of sediment size to deposit thickness is obvious. A regression analysis on the data was performed and shows a power law relationship as $a = 1.46(d_{50}/t_s)^{0.74}$. On the contrary, the power law b is independent on the d_{50}/t_s ratio, and it can be said (by averaging the b values for all set of data except for $t_s = d_{50}$) that $b \sim -0.29$. In comparison, the averaged coefficient b obtained in this study is much lower than the values obtained in the works of Novak & Nalluri (1975) and El-Zaemey (1991).

Substituting the relation of a into Equation (4), a better accuracy to find the critical velocity for sediment deposit in a rigid pipe is presented as

$$F_{d,c} = \frac{U_c}{\sqrt{gd(s-1)}} = 1.46 \left(\frac{d_{50}}{t_s} \right)^{0.74} \left(\frac{d_{50}}{y_0} \right)^{-0.25}. \quad (5)$$

3.3. Comparison of Empirical Equations

The performance of predicted F_d , obtained from Equation (5) is assessed by comparing with calculated F_d through the Novak & Nalluri (1984) and El-Zaemey (1991) equations. Fig. 6 shows that the developed equation managed to well incorporate the effect of sediment bed thickness. Despite overestimation, at larger F_d (that is at lower thickness), the equation is able to provide an accurate F_d (hence, critical velocity) value at higher sediment thickness. Most of the data falls close to the line of agreement. This is useful as the thickness of the sediment deposit in rigid pipes (or open channels) is often much larger than the median grain size d_{50} .

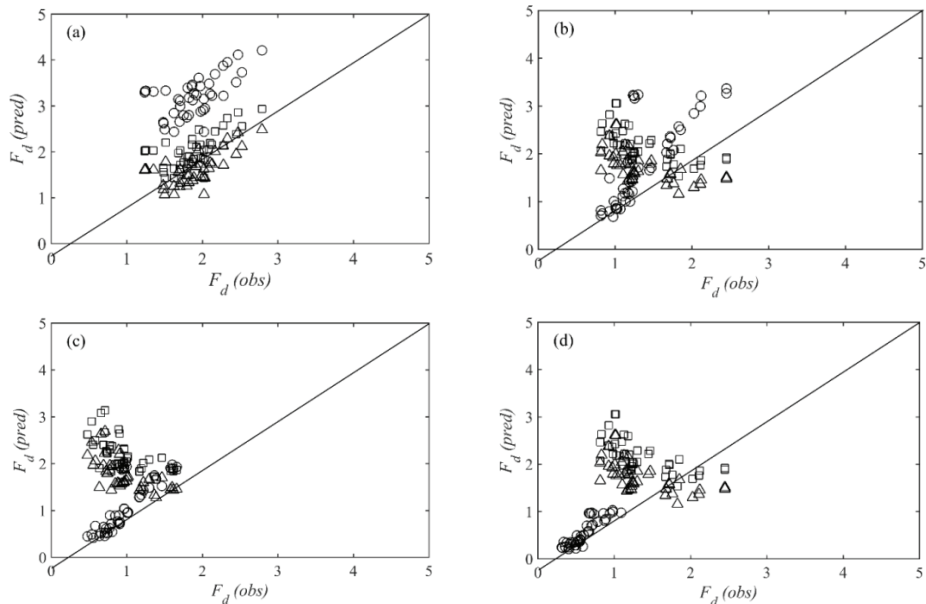


Fig. 6 - The performance of predicted F_d based on El-Zaemey's (\square), Novak's (\triangle) and proposed equations (i.e. Eq. 5) (\circ) for bed thicknesses of (a) d_{50} , (b) 5 mm, (c) 10 mm and (d) 24 mm.

Interestingly, Fig. 6 (a) shows that the prediction of F_d through both Novak and Nalluri (1984) and El-Zaemey (1991) equations work well for higher F_d , where the data points coincide well with the line of agreement. On the contrary, calculated F_d for $t_s = d_{50}$ is consistently overestimated, and deviates from the line of agreement. Therefore, to analyse the influence of bed depth, the data is revisited and individually plotted according to the sediment thickness to determine the feasibility of both El-Zaemey and Equation (5), shown in Fig. 6 (b), (c) and (d) for $t_s = 5, 10$ and 24 mm, respectively.

Data in Fig. 6 shows that the prediction of F_d is good when using both Novak and Nalluri's and El-Zaemey's equations for $t_s = d_{50}$. It is worthwhile to highlight that although both equations provide similar efficiency (based on the concentrated values close to the line of agreement), the El-Zaemey based F_d are slightly overestimated whilst the Novak and Nalluri equation on the other hand underestimated the F_d .

However, as thickness increases and the ratio $\frac{d_{50}}{t_s} < 1$, the suitability of Novak and Nalluri's and El-Zaemey's equations diminishes where calculated F_d by Equation (5) proved to have better prediction. In Fig. 6(c), where thickness is 10 mm, the critical Froude number calculated using Equation (5) lies well on the line of agreement. The validity of developed Froude number equation becomes more evident at higher bed thickness (or low grain-bed ratio), where the prediction values are concentrated on the line of agreement. Values calculated using both Novak and Nalluri's and El-Zaemey's equations, on the contrary, deviated from the line of agreement. It is interesting to observe that F_d using both Novak and

Nalluri's and El-Zaemey's equations are mostly overestimated up to three times more, in particular for thicker deposition at $t_s \geq 5$ mm.

Based on the analysis, this study proposed the calculation of critical velocity (through Froude number) for rigid pipes as

$$F_d = 0.75 \left(\frac{d_{50}}{R} \right)^{-0.34} \quad \text{for } t_s = d_{50} \text{ and,} \\ F_d = 1.46 \left(\frac{d_{50}}{t_s} \right)^{0.74} \left(\frac{d_{50}}{y_0} \right)^{-0.25}, \quad \text{for } t_s > d_{50}. \quad (6)$$

The subjectivity of the definition of sediment incipient motion that is based on the interpretation of a researcher is believed to be one of the elements in the deviation of available equations. This study described the parameter F_d based on the incipient sediment motion as adopted by Novak and Nalluri (1984), whereas El-Zaemey (1991) presented the limitation of movement is based on the threshold of sediment deposition in sewer pipes. The Shields entrainment curve (which furnishes the value of θ_c) for a range of sediment when described based on initial deposition criteria, lies above the trend obtained based on incipient motion (Safari et al., 2014).

4. CONCLUSIONS

In this paper, the threshold criteria of sediment motion with varying sediment thickness t_s ranging from d_{50} to 50 mm is reported. Using a set of homogeneous sediment with diameters from 0.55 mm to 4.75 mm, a series of experiments were conducted to obtain the critical mean velocity U_c for sediment movement. Attention was also focused on evaluating the Shields curve, whereby the shear critical velocity u_{*c} was expressed using the bed-slope product and log law. Both sets of data displayed underestimation of critical Shields parameter θ_c , which is well below the traditional Shields curve. Increasing sediment thickness was found to subsequently increase the θ_c , particularly for lower Reynolds particle number D_* , whereas for higher sediment size, a relatively constant θ_c was observed and can be said to be independent of t_s .

We also expressed the threshold criteria based on the increasingly received attention parameter of particle critical Froude number F_d to obtain the mean critical fluid velocity U_c . A higher value of U_c is needed for smaller sediment thickness and decreased as the thickness gets bigger. For smaller t_s , U_c exponentially increased as the sediment size got bigger but the big variation of U_c lessen as the sediment bed gets thicker. The effect of sediment bed thickness is rather evident and should be taken into account in the engineering design, particularly in the determination of self-cleansing velocity in rigid pipes.

Acknowledgments

The first author thanks the Ministry of Higher Education for the Fundamental Research Grant Scheme FRGS/1/2018/TK01/UKM/02/4 and the second author expresses gratitude to Universiti Malaysia Sarawak for financial support under the MyRA Special Grant Scheme (Grant No.: F02/SpGS/1542/2017).

References

- [1] Ab. Ghani, A., Zakaria, N. A., Kassim, M. and Nasir, B. A. Sediment size characteristics of urban drains in Malaysian cities. *Urban Water Journal*. 2(4):335341, 2000.
- [2] Ahyerre, M., Chebbo, G., and Saad, M. Nature and dynamics of the water sediment interface in combined sewers. *J. Environ. Eng. ASCE*. 127(3):233239, 2001.
- [3] Ashley,R. M., Wotherspoon, D. J. J., Coghlan, B. P. and McGregor, I. The erosion and movement of sediments and associated pollutants in combined sewers. *Water Science and Technology*. 25:101-114, 1992.
- [4] Ashley, R. M., Bertrand-Krajewski, J.-L., Hvítved-Jacobsen, T. and Verbanck, M. Solids in Sewers Characteristics, Effects and Control of Sewer Solids and Associated Pollutants. IWA Publishing, London, 2004.
- [5] Banasiak, R., Verhoeven, R., De Sutter, R. and Tait, S. The erosion behaviour of biologically active sewer sediment deposits: Observations from a laboratory study. *Water Research*. 39:5221-5231, 2005.
- [6] Bong, C. H. J., Lau, T. L., and Ab. Ghani, A. Verification of Equations for Incipient Motion Studies for a Rigid Rectangular Channel. *Water Science and Technology*. 67(2):395-403, 2013.
- [7] Bong, C. H. J., Lau, T. L. and Ab. Ghani, A. Sediment size and deposition characteristics in Malaysian urban concrete drains-a case study of Kuching city. *Urban Water Journal*. 11(1):74-89, 2014.
- [8] Bong, C. H. J., Lau, T. L., Ab. Ghani, A. and Chan, N.W. Sediment deposit thickness and its effect on critical velocity for incipient motion. *Water Science and Technology*. 74(8):1876-1884, 2016.
- [9] Brownlie, W. Prediction of flow depth and sediment discharge in open channels. Tech. Rep. No. Report No. KH-R-43A. Pasadena, California: California.Inst. Tech., 1981.
- [10] Buffington, J. M. and Montgomery, D. A systematic analysis of eight decades of incipient motion studies, with special reference to gravel-bedded rivers. *Water Res. Res.* 33:19932029, 1997.
- [11] Cheng, N. and Emadzadeh, A. Estimate of sediment pickup rate with the densimetric Froude number. *Journal of Hydraulic Engineering*. 06015024, 2015.
- [12] Crabtree, R.W. Sediments in sewers. *J. Inst. Water Environ. Manage.* 3:569578, 1989.
- [13] El-Zaemey, A. K. S. Sediment Transport Over Deposited Bed Sewers. PhD Thesis, University of Newcastle upon Tyne, 1991.
- [14] Kramer, H. Sand mixtures and sand movement in fluvial models. *Transaction, ASCE*. 100:798-878, 1935.
- [15] McLellan, S.L., Roguet, A. The unexpected habitat in sewer pipes for the propagation of microbial communities and their imprint on urban waters. *Current Opinion in Biotechnology*, 57, 34-41, 2019.

- [16] Novak, P. and Nalluri, C. Sediment transport in smooth fixed bed channels. *Journal of the Hydraulics Division*. 101:1139-1154, 1975.
- [17] Novak, P. and Nalluri, C. Incipient motion of sediment particles over fixed beds. *Journal of Hydraulic Research*. 22(3):181-197, 1984.
- [18] Regueiro-Picallo, M., Anta, J., Suarez, J., Jeronimo, P., Jacome, A., Naves, J. Characterization of sediments during transport of solids in circular sewer pipes. *Water Science Technology*, 2017(1), 8-15, 2018.
- [19] Safari, M.J.S., Mohammadi, M., Gilanizadehdizaj, G. On the effect of cross sectional shape on incipient motion and deposition of sediments in fixed bed channels. *J. Hydrol. Hydromech.*, 62(1), 7581, 2017.
- [20] Safari, M. J. S., Aksoy, H., Unal, N. E., Mohammadi, M. Experimental analysis of sediment incipient motion in rigid boundary open channels. *Environmental Fluid Mechanics*, 17(6), 1281-1298, 2017.
- [21] Salem, A. M. Incipient motion over loose deposited beds in a rigid rectangular channel, MSc. thesis, Universiti Sains Malaysia, 1998.
- [22] Shields, A. Anwendung der ahnlichkeitsmechanik und der turbulentzorschung auf die geschiebebewegung. PhD, Mitt. Preuss. Versuchsanst. Wasserbau Schiffbau, 1936.
- [23] Schertzinger, G., Zimmermann, S., Sures, B. Predicted sediment toxicity downstream of combined sewer overflows corresponds with effects measured in two sediment contact bioassays. *Environmental Pollution*, 258, 782-791, 2019.
- [24] Seco, I., Schellart, A., Gomez-Valentin, M., Tait, S. Prediction of Organic Combined Sewer Sediment Release and Transport. *Journal of Hydraulic Engineering*, 144(3), 1-14, 2018.
- [25] Shvidchenko, A. B. Incipient Motion of Streambeds. PhD thesis, University of Glasgow, Glasgow, UK, 2000.
- [26] Tait, S.J., Rushforth, P.J., Saul, A.J. A laboratory study of the erosion and transport of cohesive-like sediment mixtures in sewers. *Water Sci. Technol.* 37 (1):163170, 1998.
- [27] Toriman, M.E., Kamarudin, M.K.A., Idris, M., Jamil, N.R., Gazim, M.B., Abd Aziz, N.A. Sediment concentration and load analyses at Chini River, Pekan, Pahang, Malaysia. *Research Journal of Earth Sciences*, 1:43-50, 2009.
- [28] Toriman, M.E., Ata, F.M., Mohd, K., Idris, M. Bedload sediment profile and effect of river bank erosion on river cross-section. *American Journal of Environmental Sciences*, 9(4):292-300, 2013.
- [29] Verbanck, M. A., Ashley, R. M., Bachoc, A. International workshop on origin, occurrence and behaviour of sediments in sewer systems: summary of conclusions. *Water Research*. 28(1):187-194, 1994.
- [30] Vollertsen, J. and Hvítved-Jacobsen, T. Resuspension and oxygen uptake of sediments in combined sewers. *Urban Water*. 2:21-27, 2000.
- [31] Yalin, M.S. *Mechanics of Sediment Transport*. Pergamon, New York, 1972.

- [32] Wan Mohtar, W.H.M. Junaidi, Sharil, S., Mukhlisin, M. Representative sediment sizes in predicting the bed-material load for non-uniform sediments. International Journal of Sediment Research. 31:79-86, 2016.
- [33] Wan Mohtar, W.H.M. Enhanced understanding on incipient sediment motion and sediment suspension through oscillating-grid turbulence experiments. J Zhejiang Univ-Sci A (Appl Phys & Eng). 18(11):882-894, 2017.
- [34] Wan Mohtar, W.H.M. and R.J. Munro. Threshold criteria for incipient sediment motion on an inclined bedform in the presence of oscillating-grid turbulence. Phys. Fluids. 25:015103, 2013.